Biointerface Research in Applied Chemistry
Open-Access Journal (ISSN: 2069-5837)

Article
Volume 13, Issue 1, 2023, 7
https://doi.org/10.33263/BRIAC131.007

A Synergistic Broad-Spectrum Viral Entry Blocker: *In-Silico* Approach

Priyank Purohit [1,*], Ravi K Mittal [1,2], Vikram Sharma [3]

[1] Department of Pharmacy, HIMT, Gautam Buddh Nagar, Greater Noida, Uttar Pradesh, 201308, India; priyank.niper@gmail.com (P.P.);
[2] Department of Natural Product, National Institute of Pharmaceutical Education and Research (NIPER), Sector-67, SAS Nagar, Punjab-160062, India
[3] Galgotias College of pharmacy, Greater Noida, Uttar Pradesh, 201308, India
* Correspondence: priyank.niper@gmail.com (P.P.);

Scopus Author ID: 56149543500
Received: 8.10.2021; Accepted: 7.11.2021; Published: 7.01.2022

Abstract: Increasing victims of viral attacks is a serious concern of the current time as well as soon. The story of virulence was started with the origin of the Spanish flu pandemic of 1918, later severe other viral infections like SARS, MARS, and many others took the life of many people. Currently, the situation is locked in the world because of the unprecedented arrival of the COVID-19 from the Wuhan, city of China. The current need turned to make suitable candidates with the existing safety data, to get the molecule in a limited period. Because of that, the quinolone 3-carboxy derivatives were docked with many targets enzyme, but the interaction with gp-41 was found interactive, which is represented with interactive binding energy scores. In this regard, the validated target of the virus likes HIV. COVID-19 and other viruses were utilized to see the beneficial interactions. The present research is based on the Quinoline-3carboxy derivatives and their interaction with gp41. The gp41 has been found with the highest similarity with the S2 protein of the Coronavirus; targeting this protein will inhibit the interaction of cells and viruses. The *in silico* results were found encouraging with the suitable interactions with the amino acid residues. The results give us the hope to develop a lead for the inhibition of viral infection, including HIV, flu, and Coronavirus. The result is summarized with all the *in silico* docking and residual interaction with the reasonable concept of lead to go further in the drug discovery process

Keywords: anti-COVID; entry blocker; broad-spectrum anti-viral.

1. Introduction

A virus completes its lifecycle with the four essential steps, viral entry through fusion, RNA replication, assembly, and release [1]. The entry of viruses inside the host cell is crucial for replicating and transmitting the virus to the neighbor cell. The entry of the virus is mediated by the spike protein, which binds with the angiotensin-converting enzyme 2 (ACE2) of the human cell in the case of the SARS-CoV-2, while other interacts with the different enzyme targets [2]. Recently our group published the activity of 2-styryl quinoline derivatives with 3-ester [3] and their hydrolyzed derivatives, with their high selectivity [4] (compound 1, Figure 1), which was also represented as DNA minor groove binding agents [5]. These compounds were utilized for the *in silico* interactions. However, the specific interaction with gp-41 is represented a claimed as wide spectrum viral entry blockers.

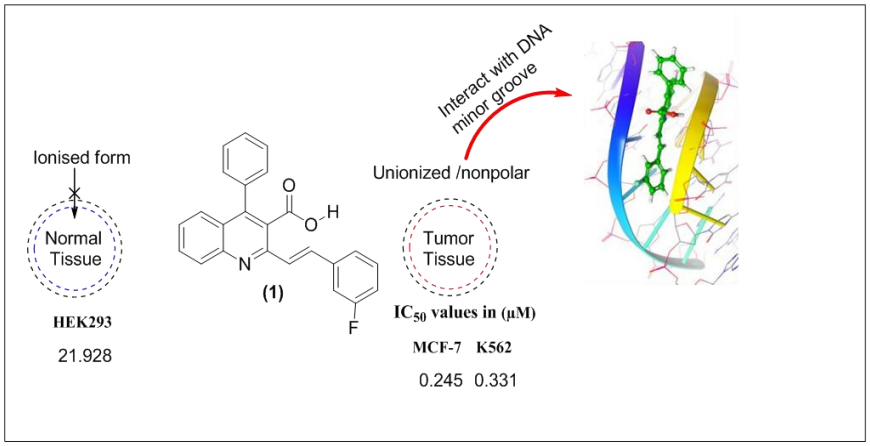

Figure 1. Quinine derivatives as an anti-proliferating agent.

1.1. Fusion of virus with host cell.

The surface spike glycoprotein consists of three S1-S2 heterodimers parts, with the receptor-binding domain, which was revealed on the subdomain of S1 and initiate the infusion of the virus through binding with the cellular receptor ACE-2 [6]. Cell fusion and entry are crucial phenomena of the virus, which govern the host's morbidity and mortality. The fusion is a result of the conformational changes of the spike molecule, which enable the virus to invade into the host cell and initiate replication [7]. The reasonable factor for the fusion proteins of SARS-CoV revealed as highly similar to gp41 from human immunodeficiency virus, hemagglutinin (HA) from influenza [8], and the paramyxovirus [9], which makes this hypothesis towards broad-spectrum anti-viral [10].

1.2. Fusion inhibitors.

The infusion of the virus into the cell creates an opportunity to take the host cell's resources, grow inside and transfuse outside from the host cell to enhance the viral load in the host body. In view of that, the treatment strategy should emphasize the entry or infusion, which will rarely disturb the host cell's essential physiology, and avoid the anti-viral drug's most concern problem.

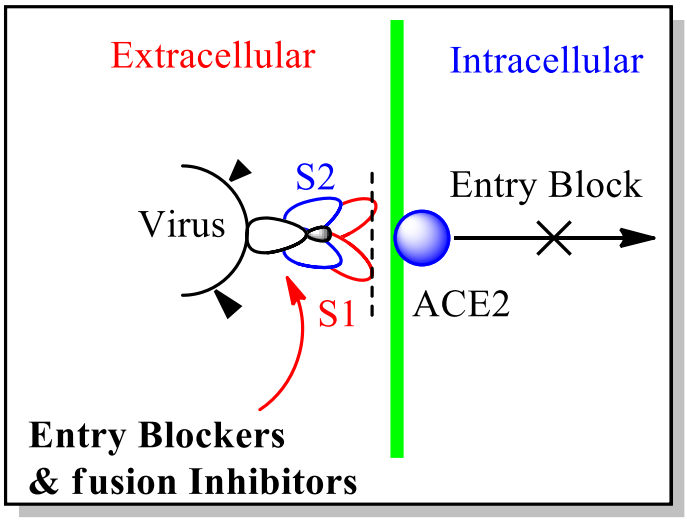

Figure 2. Binding of Fusion inhibitors in the spike protein.

The entry of a virus inside the host cell compromises the cytoplasmic transport systems to move the replication sites within the cytosol for RNA viruses and the nucleus for DNA

viruses. The replication of genetic material starts with the final step of viral entry, which proliferates the genome to get in the shape through the transfusion from the host cell [11]. As infusion inhibitors/ entry blockers, anti-viral therapies have been an attractive target. Moreover, many research scientists revealed many targets like S protein include RBDeACE2 blockers, S cleavage inhibitors, fusion core blockers, neutralizing antibodies, protease inhibitors, S protein inhibitors, and small interfering RNAs (Figure 2). Among them all, a US FDA approved (2003) "Enfuvirtide" as entry blocker of HIV-1 virus with the gp41 derived peptide (INN) [12].

1.3. Structural of gp41.

Zhang *et al*. (2004) reported the structural similarity between HIV-1 gp41 and SARS-CoV S2 proteins and found that they shared the same two α helices, facilitating the virus's entry into the host cell. The infusion of the virus into the cell creates an opportunity to inhibit viral replication and aggregation, as depicted in Figure 3 [13].

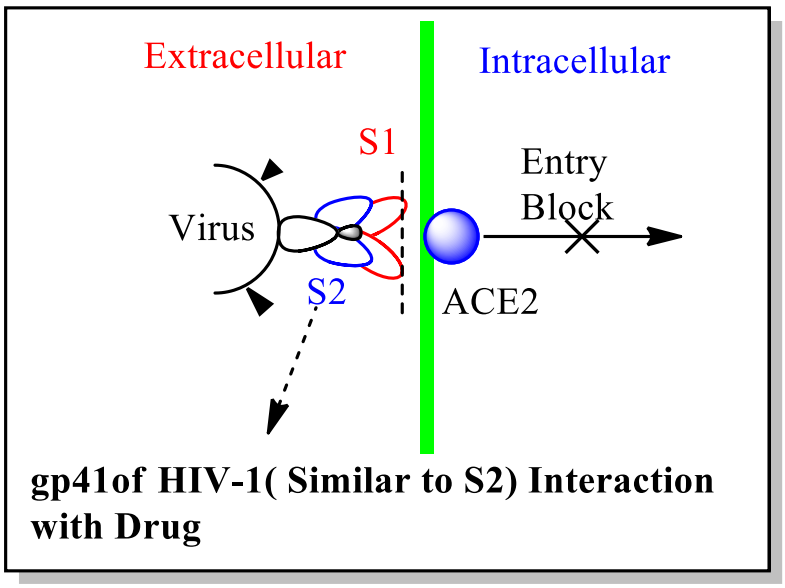

Figure 3. S2 protein as a target for infusion inhibitors.

Here, the gp41 of HIV-1 target is used for the docking and molecular interaction. The genomic resemblance of both targets has an advantage: both viruses could be blocked from the entry point.

2. Materials and Methods

2.1. Docking.

All the synthesized derivatives were docked against, validated HIV-1 based gp41protein to determine the mechanism of action that will benefit further for designing molecules to act/bind on the same target.

2.2. Preparation of proteins.

AutoDock Tool was used to prepare proteins gp41, as PDB ID "1AIK'. In the active site, ligands and water molecules were removed while the charge of magnesium was kept +2. The merger of nonpolar hydrogens, the addition of Kollman charges, and assignment for AutoDock atom type were done [17-19].

2.3. Preparation of ligands.

The ligand was prepared using the AutoDock tool while its structure was made using ChemBioDraw Ultra software. Merging nonpolar hydrogens, adding Gasteiger charges, and assignment for AutoDock atom type were done while energy minimization was achieved with MOPAC using the PM3 method [20-22].

2.4. Docking interaction.

Molecular docking, an important method in structure-based computer-assisted drug design, predicts a ligand's main binding mode(s) with a protein of known three-dimensional structure [23]. From another aspect of view, docking simulation could be applied to find the binding mode and mechanism of more active derivatives. Molecular docking simulation of the interaction with gp41 was carried out to investigate the possible inhibition of this protein with the designed compounds [24-26]. The safety *in silico* and QED results were encouraging, which gave a logistic approach to define the way to see against the similar target of viral [27-29]. The drug-likeness value was calculated through QED value, and the value was calculated for all the synthesized compounds **1(a-m)** and **2(a-p)**. These compounds were screened as per their drug-likeliness value, which was assessed physicochemical using Lipinski's rule of five (ro5) along with the QED value; ADME results were found superior to get the best outcome of the synthesized compounds [30-33].

3. Results and Discussion

3.1. Common interaction of quinoline-3-carboxylate with the active site of gp41 HIV-1.

In the initial stage, a prototype of the 2-Styryl 3-carboxylate quinoline compound **1m** was docked for the *in silico* drug enzyme activity; the results are summarized below with the all-possible interactions. The further various derivatives were screened for *in silico* anti-viral activity (Figure 4), with the active site of gp41 (HIV-1).

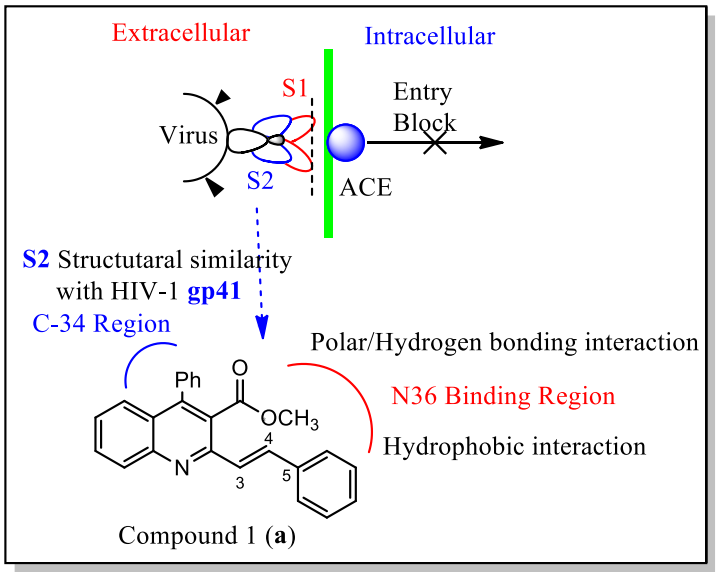

Figure 4. Interaction of Quinoline derivative and gp41.

3.1.1. Interaction at N36 (546-581) chain.

Hydrophobic interactions: GLN 550, 551, 552 LEU 555, ARG 557, ALA 558, GLU 560

Hydrogen bonding: C=O----H-O-GLN 562

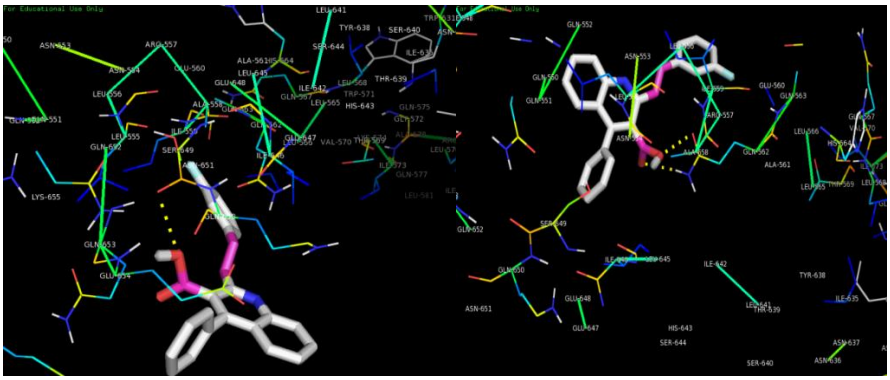

Figure 5. Interaction at N36 chain of hex helical.

3.1.2. Interaction at C34 (628-660) site.

Hydrophobic interactions: ILE 646, GLN650, ASN 651, and 656
Hydrogen bonding: C=O----H-O-GLN 653 and SER 649

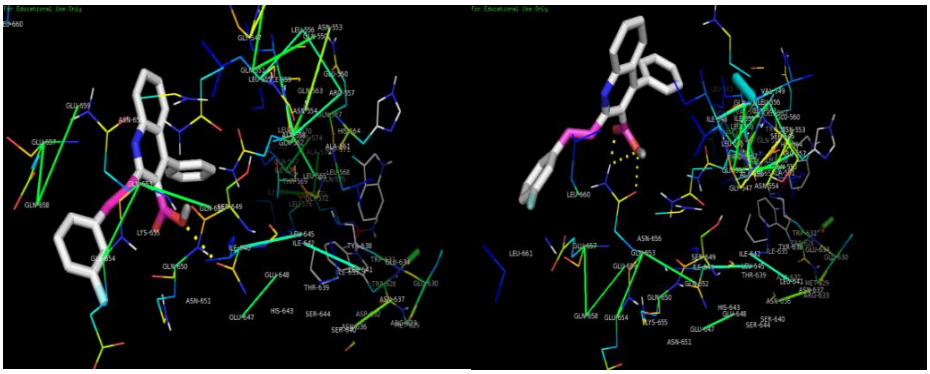

Figure 6. Interaction at C34 chain of hex helical.

The avidity of the optimization study of the interactions was started with the different substitutions of the Quinoline 3-esters and acids. The close similarity with the corona spike protein is a matter of concern in the present research. The complete *in silico* analysis of the substituted pharmacophore is below given with the list of interacting amino acid residues. The designed quinoline derivatives (Figure 7, 1 a-p) ester derivatives were docked into the active site of gp41. Docking results are summarized in Table 1.

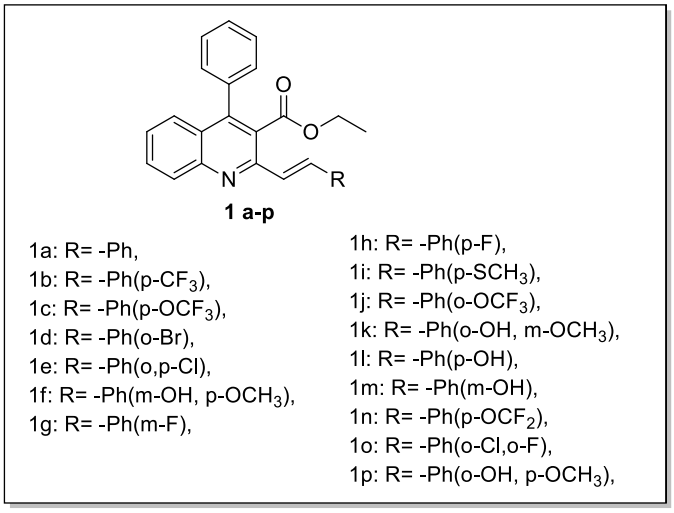

Figure 7. Structure of quinoline-3-carboxylate (**1a-p**) derivatives.

Observed binding modes were associated with different docking scores. The obtained results showed that the docked compounds were located in a groove containing due to the Hydrophobic region of the amino acid at N-36 region of gp41, which includes the GLN 550, 551, 552 LEU 555, ARG 557, ALA 558, GLU 560residues and C-34 grooves includes ILE 646, GLN 650, ASN 651, and 656 (Table 1).

Table 1. Molecular docking studies of (*E*)-ethyl-2-(2-substitutedstyryl)-4-phenylquinoline-3-carboxylate derivatives **1a-p** on gp41.

Compounds	GP41	Compounds	GP41
1a	-7.07	**1i**	-6.15
1b	-5.68	**1j**	-5.9
1c	-5.68	**1k**	**-7.78**
1d	**-7.31**	**1l**	-6.64
1e	-6.75	**1m**	-6.86
1f	-5.9	**1n**	-5.53
1g	-6.92	**1o**	-7.2
1h	-6.88	**1p**	-6.25

However, some of the compounds with a hydroxyl group (compound **1f and 1p)** were aligned towards the amino acid (ARG) through the one additional hydrogen bonding interaction, in results, those were showing better affinity than the rest of the compounds, the interaction is depicted in below Figure 8.

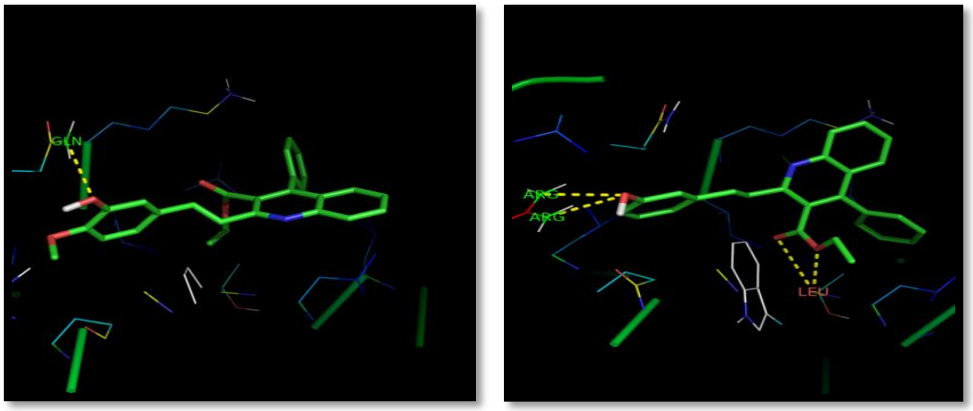

Figure 8. Docking Interaction of Compounds with better binding affinity compound (**1f** and **p).**

The surface interaction pose of the compounds **1** and enzyme showed the W shape interaction pose (Figure 9) inside the cavity of the gp41. The W shape and their aryl orientation toward the C-34 region justify the perfect binding of the compounds.

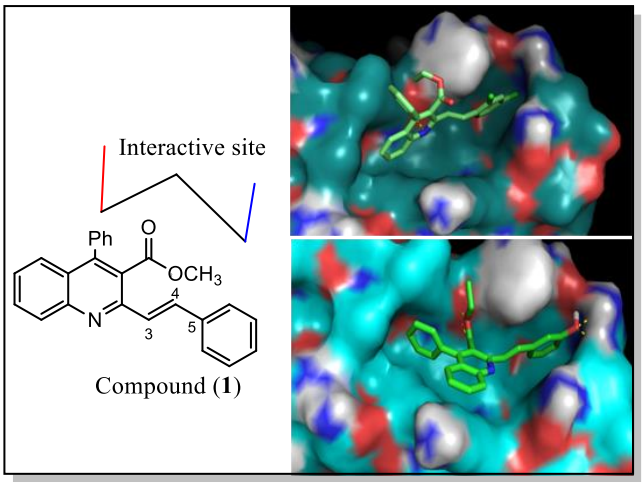

Figure 9. Binding interaction pose of compounds (**1e** and **1m**).

The best fitted with the highest binding affinity was observed with compound 1k. The additional features were investigated further with the hydrolyzed state, along with the all-hydrolyzed molecules.

3.2. Hydrolysis of ester compounds.

The non-ionized/nonpolar form can enter the cell passively, while the ionic remain outside; it was found similar in the case of ester and acid. (Figure 10) The change in pH value accumulates the drug in the infectious site more than the normal, which will automatically enhance the selectivity of the drug over the noninfectious cell [18-19].

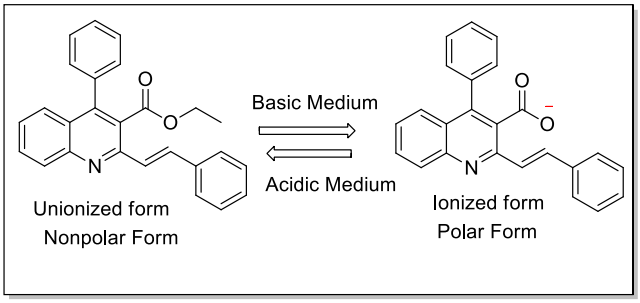

Figure 10. Different forms of the compounds in Different pH.

In view of the selectivity, the hydrolyzed compounds **2 (a-m)** (Figure 11**)** were also docked, with the score that is summarized in the below-given Table 2

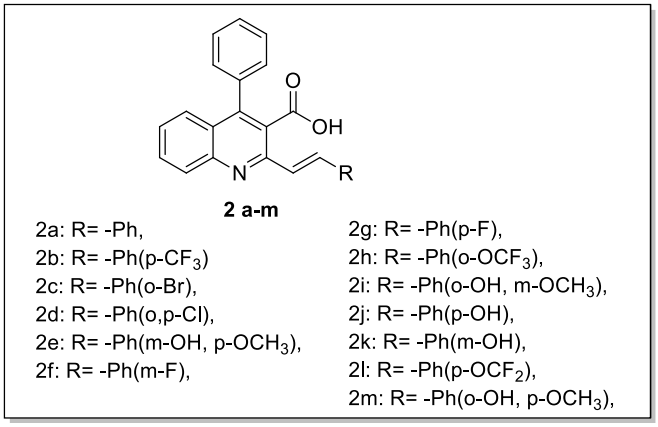

Figure 11. Structure of Series 1 quinoline-3-carboxylic acid derivatives.

These designed *(E)*-2-(substituted styryl)-4-phenylquinoline-3-carboxylic acid derivatives have been docked for the GP41 using AutoDock4. These derivatives have shown moderate to excellent binding to the active site of gp41, as shown in Table 2. The activity pattern was similar to the parent ester compounds.

Table 2. Molecular docking studies of *(E)*-2-(substituted styryl)-4-phenylquinoline-3-carboxylic acid derivatives **2a-m** on1AIK

Compounds	gp41	Compounds	gp41
2a	**-6.27**	**2h**	**-6.11**
2b	**-5.92**	**2i**	**-7.87**
2c	**-6.82**	**2j**	**-6.03**
2d	**-6.73**	**2k**	**-6.76**
2e	**-5.97**	**2l**	**-5.49**
2f	**-6.34**	**2m**	**-6.06**
2g	**-6.29**		

The *in silico* analysis of hydrolyzed compounds **2** (**a-m**) (Figure 12) was docked to the optimized gp-protein, confirming the similar interaction pattern and alignment. A similar interaction with the hydrophobic region of the amino acid at N-36 of GLN 550, 551, 552 LEU 555, ARG 557, ALA 558, GLU 560 residues and with C-34 based amino acid-like ILE 646, GLN 650, ASN 651, and 656. The W shape and their aryl orientation toward the C-34 region make the compounds the best fit. A similar analysis was also confirmed with the hydroxyl bearing functional group like compound **2i** makes the additional hydrogen bonds with the amino acid, which elevate the drug's efficacy, as given in below tables and figures.

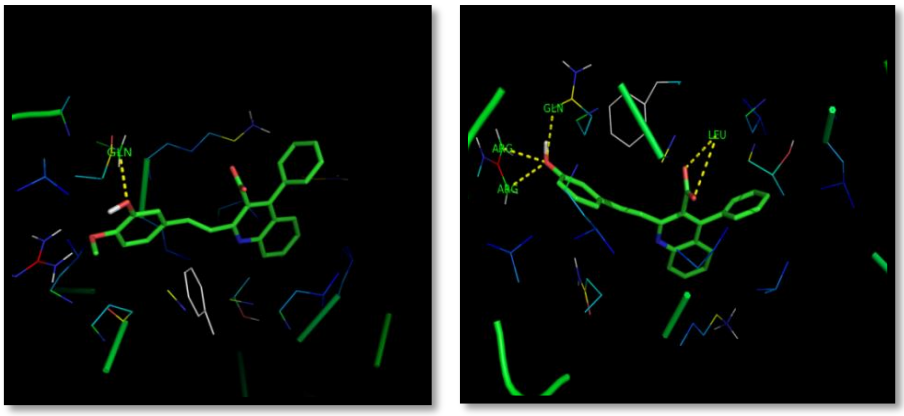

Figure 12. Docking Interaction of Compound 2e, and k.

The drug and enzyme's surface interaction inside the cavity gave a similar alignment of the active docked compounds as it was showing with the easter parent compounds. The hydrolyzed product gives the same topological interaction and alignment inside the cavity of gp41.

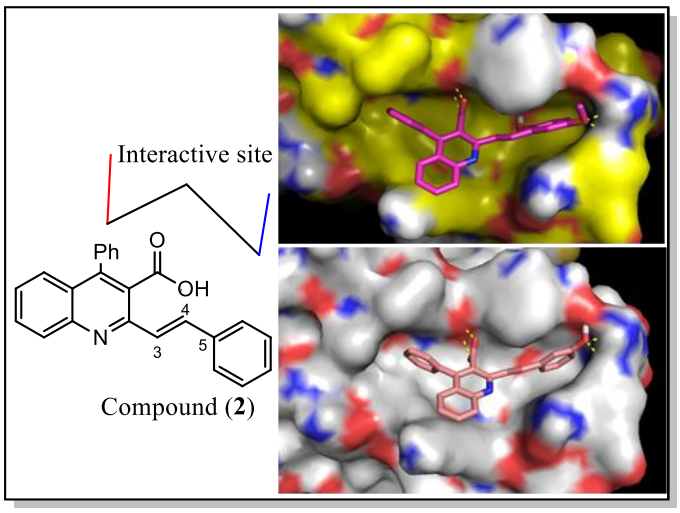

Figure 13. Docking Interaction of Compound **2i**, and **2k** with gp-41.

In conclusion, the quinoline compounds showed the activity inside the active site of the gp-41, with their W-shaped pose and specific interaction with the N-36 and C-34 site of the six helical structures of the gp-41infusion protein. The additional interaction with the ARG makes some compounds more potent, like compounds 1k and 2i (Figure 14).

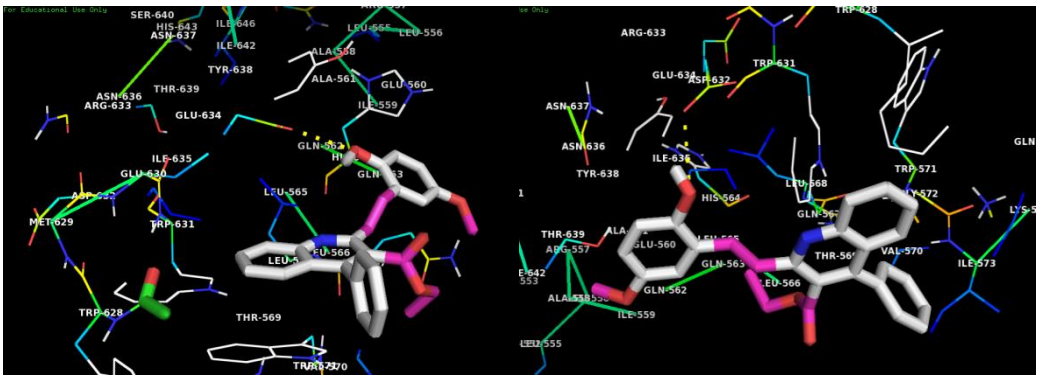

Figure 14. Docking Interaction of Compound**1k** and**2i** with gp41.

Moreover, compound **2i,** with lower pKa values, will show selectivity toward the virus because of the acidic surroundings in the virus-infected area, which eventually decreases the toxicity to the normal cell. (Figure 15).

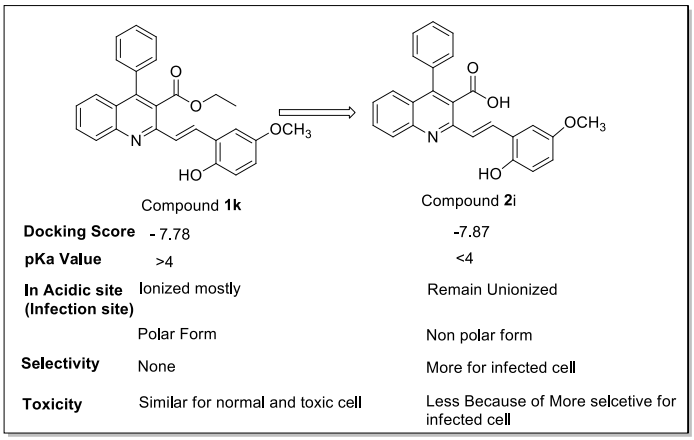

Figure 15. Different forms of the compounds in different pH.

4. Conclusions

All the QED and toxicity predictions found it favorable for the compounds to act like drug molecules. The interaction with gp41 makes the wider scope of the viral with their privileged anticancer activity. The future development scope for the drug *in vitro* evaluation will be crucial to the drug development process. The *in silico* study gives the initial hint of the molecule about their future drug candidates' wide spectrum anti-viral agents.

Funding

This research received no external funding

Acknowledgments

We acknowledge the initial support from DBT: BT/PR5634/MED/29/623/2012 and ICMR: 5/7/827/12-RCH and Dr. K. K Bhutani (NIPER Mohali) for the Ph.D. project of RKM. A special thanks to "Preserve Creativity Pvt. Ltd" for providing a creative space to finalize the data.

Conflicts of Interest

The authors declare no conflict of interest.

References

1. Weiss, S. R.; Navas-Martin, S. Coronavirus pathogenesis and the emerging pathogen severe acute respiratory syndrome coronavirus. *Microbiol. Mol. Biol. Rev*. **2005**, *69*, 635−664, https://doi.org/10.1128/MMBR.69.4.635-664.2005.
2. Xiu, S.; Dick, A.; Ju, H.; Mirzaie, S.; Abdi, F.; Cocklin, S.; Zhan, P.; Liu, X. Inhibitors of SARS-CoV-2 Entry: Current and Future Opportunities. *Journal of medicinal chemistry* **2020**, *63*, 12256-12274, http://doi.org/10.1021/acs.jmedchem.0c00502.
3. Mittal R. K.; Purohit, P. Quinoline-3-carboxylate Derivatives: A New Hope as an Antiproliferative Agent. *Anticancer Agents in Medicinal Chemistry* **2020**, *20*, 1981-1991, https://doi.org/10.2174/1871520620666200619175906.
4. Mittal R. K.; Purohit, P. Quinoline-3-Carboxylic Acids: A Step toward Highly Selective Antiproliferative Agent. *Anticancer Agents in Medicinal Chemistry* **2020**, *20*, https://doi.org/10.2174/1871520620999201124214112.
5. Mittal R. K.; Purohit, P; Khatana, K. Quinoline-3-Carboxylic Acids DNA Minor Groove-Binding Agent. *Anticancer Agents Med Chem.* **2021**, https://doi.org/10.2174/1871520621666210513160714.
6. Kong, R.; Yang, G.; Xue, R.; Liu, M.; Wang, F.; Hu, J.; Guo, X.; Chang, S. COVID-19 Docking Server: a meta server for docking small molecules, peptides and antibodies against potential targets of COVID-19. *Bioinformatics (Oxford, England)* **2020**, *36*, 5109-5111, http://doi.org/10.1093/bioinformatics/btaa645.
7. Kliger, Y., Levanon, E. Y. Cloaked similarity between HIV-1 and SARS-CoV suggests an anti-SARS strategy. *BMC microbiology* **2003**, *3*, 20, https://doi.org/10.1186/1471-2180-3-20.
8. Beniac, DR.; Andonov, A.; Grudeski, E.; Booth, TF. Architecture of the SARS coronavirus prefusion spike. *Nat Struct Mol Biol.* **2006**, *13*, 751-752, https://doi.org/10.1038/nsmb1123.
9. Lu, M.; Blacklow, S.C.; Kim, P.S. A trimeric structural domain of the HIV-1 transmembrane glycoprotein. *Nature Struct. Biol*. **1995**, *2*, 1075–1082, https://doi.org/10.1038/nsb1295-1075.
10. Armand-Ugón, M.; Gutiérrez, A.; Clotet, B.; Esté, JA. HIV-1 resistance to the gp41-dependent fusion inhibitor C-34. *Antivir. Res.* **2003**, *59*, 137-42, https://doi.org/10.1016/s0166-3542(03)00071-8.
11. Yamauchi, Y.; Helenius, A. Virus entry at a glance. *Journal of cell science* **2013**, *126*, 1289-1295, http://doi.org/10.1242/jcs.119685.
12. Fung, H. B., & Guo, Y. Enfuvirtide: a fusion inhibitor for the treatment of HIV infection. *Clin. therap*. **2004**, *26*, 352-378, https://doi.org/10.1016/S0149-2918(04)90032-X
13. Wu Zhang, X.; Leng Yap, Y. Structural similarity between HIV-1 gp41 and SARS-CoV S2 proteins suggests an analogous membrane fusion mechanism. *Theochem* **2004**, *677*, 73-76, http://doi.org/10.1016/j.theochem.2004.02.018.
14. Cheng, F.; Li, W.; Zhou, Y.; Shen, J.; Wu, Z.; Liu, G.; Lee, P. W.; Tang, Y. admetSAR: a comprehensive source and free tool for assessment of chemical ADMET properties. *J. Chem. Inf. Model.* **2012**, *52*, 3099–3105, https://doi.org/10.1021/ci300367a.
15. A comprehensive source and free tool for evaluating chemical ADMET properties. http://lmmd.ecust.edu.cn/admetsar1/ (18 March 2016).
16. Morris, G.M.; Huey, R.; Lindstrom, W.; Sanner, M.F.; Belew, R.K.; Goodsell, D.S.; Olson, A.J. AutoDock4 and AutoDockTools4: Automated docking with selective receptor flexibility. *J. Comput. Chem.* **2009**, *30*, 2785-2791, https://doi.org/10.1002/jcc.21256.
17. Liu, H.; Maruyama, H., Masuda, T.; Honda, A.; Arai, F. The influence of virus infection on the extracellular pH of the host cell detected on cell membrane. *Front. Microbiol.* **2016**, *7*, 1127, https://doi.org/10.3389/fmicb.2016.01127.
18. Dankó T.; Hargitai D.; Pataki Á.; Hakim H.; Molnár M.; Zsembery Á. Extracellular alkalinization stimulates calcium-activated chloride conductance in cystic fibrosis human airway epithelial cells. *Cell. Physiol. Biochem*. **2011**, *27* (3-4), https://doi.org/10.1159/000327967.
19. Luo, L.; Qiu, Q.; Huang, F.; Liu, K.; Lan. Y.; Li, X.; Huang, Y.; Cui, L.; Luo, H. Drug repurposing against coronavirus disease 2019 (COVID-19): A review. *J. Pharm. Anal.* **2021**, https://doi.org/10.1016/j.jpha.2021.09.001.
20. Enmozhi, SK.; Raja, K.; Sebastine, I.; Joseph, J. Andrographolide as a potential inhibitor of SARS-CoV-2 main protease: An in silico approach. *J. Biomol. Struct. Dyn.* **2021**, *39*,, 3092-8, https://doi.org/10.1080/07391102.2020.1760136.

21. Dey, D.; Dey, N.; Ghosh, S.; Thiagarajan, P. In silico studies predict efficient binding of remdesivir and favipiravir with 3-chymotrypsin like protease of SARS-CoV-2 for COVID-19 interventional therapy. *Indian J. Pharm. Sci.* **2021**, *83*, 556-61, https://doi.10.36468/pharmaceutical-sciences.805.
22. Yosri, N.; El-Wahed, A.; Aida, A.; Ghonaim, R.; Khattab, OM.; Sabry, A.; Ibrahim, MA.; Moustafa, MF.; Guo, Z.; Zou, X.; Algethami, AF. Anti-viral and Immunomodulatory Properties of Propolis: Chemical Diversity, Pharmacological Properties, Preclinical and Clinical Applications, and In Silico Potential against SARS-CoV-2. *Foods* **2021**, *10*, 1776, https://doi.org/10.3390/foods10081776.
23. Norinder, U.; Tuck, A.; Norgren, K.; Kos, VM. Existing highly accumulating lysosomotropic drugs with potential for repurposing to target COVID-19. *Biomed. Pharmacother.* **2020**, *130*, https://doi.org/10.1016/j.biopha.2020.110582.
24. Chakravarty, K.; Antontsev, VG.; Khotimchenko, M.; Gupta, N.; Jagarapu, A.; Bundey Y, Hou H.; Maharao, N.; Varshney, J. Accelerated repurposing and drug development of pulmonary hypertension therapies for COVID-19 treatment using an AI-integrated biosimulation platform. *Molecules* **2021**, *26*, https://doi.org/10.3390/molecules26071912.
25. Sarhan, A.A.; Ashour, N.A.; Al-Karmalawy, A.A. The journey of antimalarial drugs against SARS-CoV-2. *Inform. Med. Unlocked* **2021**, 100604, https://doi.org/10.1016/j.imu.2021.100604.
26. Du, R.; Cheng, H.; Cui, Q.; Peet, NP.; Gaisina, IN.; Rong L. Identification of a novel inhibitor targeting influenza A virus group 2 hemagglutinins. *Antivir. Res.* **2021**, *186*, http://doi.org/10.1016/j.antiviral.2021.105013.
27. Sutanto, H.; Heijman, J. Beta-adrenergic receptor stimulation modulates the cellular proarrhythmic effects of chloroquine and azithromycin. *Front. Physiol.* **2020**, *11*, 1346, https://doi.org/10.3389/fphys.2020.587709.
28. Joshi, S.; Joshi, M.; Degani, MS. Tackling SARS-CoV-2: proposed targets and repurposed drugs. *Future Med. Chem.* **2020**, *17*, 1579-601, https://doi.org/10.4155/fmc-2020-0147.
29. Hou, Y.; Ge S, Li X.; Wang, C.; He H, He L. Testing of the inhibitory effects of loratadine and desloratadine on SARS-CoV-2 spike pseudotyped virus viropexis. *Chem. Biol. Interact.* **2021**, *338*, https://doi.org/10.1016/j.cbi.2021.109420.
30. Joshi, S.; Joshi, M.; Degani, MS. Tackling SARS-CoV-2: proposed targets and repurposed drugs. *Future Med. Chem.* **2020**, *12*, https://doi.org/10.4155/fmc-2020-0147.
31. Gorgulla, C.; Das, KM.; Leigh, KE.; Cespugli, M.; Fischer, PD.; Wang, ZF.; Tesseyre, G.; Pandita, S.; Shnapir, A.; Calderaio, A.; Gechev, M. A multi-pronged approach targeting SARS-CoV-2 proteins using ultra-large virtual screening. *Iscience* **2021**, *24*, https://doi.org/10.1016/j.isci.2020.102021.
32. Ghildiyal, R.; Gabrani R. Antiviral therapeutics for chikungunya virus. *Expert Opin Ther Pat.* **2020**, 467-80, https://doi.org/10.1080/13543776.2020.1751817.
33. Almasi, F.; Mohammadipanah, F. Hypothetical targets and plausible drugs of coronavirus infection caused by SARS-CoV-2. *Transbound Emerg Dis.* **2021**, *68*, 318-32, https://dx.doi.org/10.1111%2Ftbed.13734.